 doi:10.20944/preprints202102.0114.v1

Article

Influence of material-dependent damping on brake squeal in the specific disc brake system

Juraj Úradníček [1,*], Miloš Musil [1], Ľuboš Gašparovič [1] and Michal Bachratý [2]

1 Institute of Applied Mechanics and Mechatronics, Faculty of Mechanical Engineering, Slovak University of Technology in Bratislava, Námestie slobody 17, 812 31 Bratislava, Slovakia; juraj.uradnicek@stuba.sk (J.U.), milos.musil@stuba.sk (M.M.), lubos.gasparovic@stuba.sk (Ľ.G.)

2 Institute of Manufacturing Systems, Environmental Technology and Quality Management, Faculty of Mechanical Engineering, Slovak University of Technology in Bratislava, Námestie slobody 17, 812 31 Bratislava, Slovakia; michal.bachraty@stuba.sk

* Correspondence: juraj.uradnicek@stuba.sk

Abstract: The connection of two phenomena - non-conservative friction forces and dissipation-induced instability can lead to many interesting engineering problems. The paper studies general material-dependent damping influence on dynamical instability of disc brake systems leading to brake squeal. The effect of general damping is demonstrated on a minimal and complex model of a disc brake. A complex system including material-dependent damping is defined in the commercial finite element software. The finite element model validated by experimental data on the brake-disc test bench is used to compute the influence of a pad and a disc damping variations on system stability by complex eigenvalue analysis. Analyzes show a significant sensitivity of the experimentally verified unstable mode of the system to the ratio of the damping between the disc and the friction material components.

Keywords: brake squeal; dissipation induced instability; non-proportional damping; non-conservative system; complex eigen value analysis.

---

1. Introduction

Eigenvalue analyses to predict the stability of physical systems exposed to non-conservative forces is a current topic in engineering applications. Eigenvalues of such systems exhibit behavior depending on the amplitudes of the non-conservative forces acting on them. These dependencies lead to effects such as semisimple and nonsemisimple 1:1 resonance of the system [1]. This phenomenon is also known as Hamiltonian–Hopf bifurcation [2] or Krein Kollision [3] and in mechanical engineering terminology known as a Mode Coupling, causing flutter type instability in mechanical systems.

This phenomenon is well known in various mechanical applications where non-conservative forces play significant roles. For example, in rotary machinery with viscous damping in the shaft bearings [4], in aerodynamic systems exposed to wind flow [5], in hydrodynamic systems loaded with hydrodynamic forces [6] and last but not least in disc brake systems where friction forces are acting between a pad and a disc [7].

Non-conservative friction force brings into a brake system an undesirable phenomenon known as brake squeal. Brake squeal is a complex problem caused by the non-conservative nature of friction force, which de-symmetrizes the coefficient matrixes of mechanical systems [8]. Several different mechanisms causing brake squeal have been studied in the past decades [9], [10], but the most significant contributor to brake squeal was identified to be mode coupling. Further, the unstable behavior of mechanical systems can be caused by dissipation-induced instability, which was pointed out earlier in the work of Hoffmann [11] in the case of brake systems. In general, destabilization effect was first observed by Smith in [12], studying the stability of elastic rotors exposed to friction in bearings.

Vibration energy in brake systems is mainly dissipated due to material damping in system components and friction-induced damping between a pad and a disc [13]. Regarding the squeal prediction procedures, the finite element method (FEM) and the Complex Eigen Value analyses (CEVA) is commonly used to predict unstable vibration modes of the system [14]. To obtain a time and frequency invariant damping matrix of a FE system - represented by constant-coefficient matrixes of mass, damping, and stiffness (**M**, **C**, **K**) - material damping is commonly modeled as equivalent viscous damping characterized by damping matrix **C** constructed as a linear combination of mass **M** and stiffness **K** matrixes leading to Raylaight respectively classical system damping.

Several research studies point out that simplification of damping in the form of Rayleigh damping can be acceptable for conservative systems, but in non-conservative circulatory systems, like disk brakes, stability is given not only by the magnitude of damping but also by damping distribution over the structure. Since the friction material and the disk have an order of magnitude different damping [15], [16] and system damping is thus far from Raleigh, it is appropriate to expect dissipation-induced instability of such systems. In the case of FEM models, it means that system stability depends not only on the magnitude of damping but also on the structure of the damping coefficient matrix. The study by the Hagedorn [17] thoroughly demonstrates, on simplified examples, the influence of damping matrix structure on disc brake and paper calendar system stability. Material dependent damping optimization of full industrial FEM model of disc brake is well documented in the book [18]. However, the model doesn't consist of a physically reasonable damping factor for friction material, thus the effect of dissipation-induced instability due to different friction material and disc damping cannot be fully assessed from the study.

Despite the capabilities of modern FEM tools to model viscous damping in CEVA analyses, the damping is still not commonly included in industrial computational models for squeal prediction. This could be mainly due to two factors. First is deliberate neglecting of dissipation induced instability by anticipating purely stabilizing damping, so that undamped models appear to be on the safe side of the instability prediction. This may stem from the lack of studies that would objectively quantify the effect of damping on the dynamic instability of disc brakes. Second reason is quite complicated quantification and estimation of damping properties of given mechanical systems which can be seen from variety of measured data in various researches [16], [19]. It can be suggested that some uncertain guests have to be done to set the proper damping properties of computational models. System such as disc brake exhibits very close eigen frequencies and proper system identification tools for damping estimation should be chosen.

Based on the above information, the basic questions that the article would like to answer are:

- Can material-dependent (non-proportional) damping have a significant influence on the stability of specific disc brake structures?
- Can materially dependent damping be applied directly to computational FEM models to streamline the instability prediction process?

The questions are answered by analyzing the effect of damping on the simplified as well as the complex model of a disc brake, containing real, experimentally estimated, material and modal properties.

2. Mathematical description of disc brake minimal model

2.1. 2-DoF brake disc model

The 2-DoF brake disc model with wobbling disc is considered in this section. The model depicted on Figure 1 was introduced and analyzed by [20]. The system consists of a rigid disc rotating with angular velocity Ω that can conduct 2 independent rotations corresponding to the general coordinates q_1 and q_2. Two pins, attached to the ground by a spring element with stiffness coefficient of the pad k, represent the brake pads. Pins are perpendicular to the x_1, x_2 plane, influence only the q_1 coordinate because the pins lay on the x_2 axis, and they are in point frictional contact with rigid disc. The Coulomb's law is employed as friction model for pin-disc contact.

The equation of motion of model shown on Figure 1 is:

$$\mathbf{M}\ddot{\mathbf{q}} + \mathbf{C}\dot{\mathbf{q}} + \mathbf{K}\mathbf{q} = \mathbf{0} \tag{1}$$

where

$$\begin{aligned}
&\mathbf{M} = \begin{bmatrix} I & 0 \\ 0 & I \end{bmatrix}, \mathbf{K} = \begin{bmatrix} k_t + 2kr^2 + N_0 h & \frac{1}{2}\mu N_0 \frac{h^2}{r} \\ -\mu(khr + 2N_0 r) & k_t + (1+\mu^2)N_0 h \end{bmatrix}, \\
&\mathbf{q} = \begin{bmatrix} q_1 \\ q_2 \end{bmatrix}.
\end{aligned} \tag{2}$$

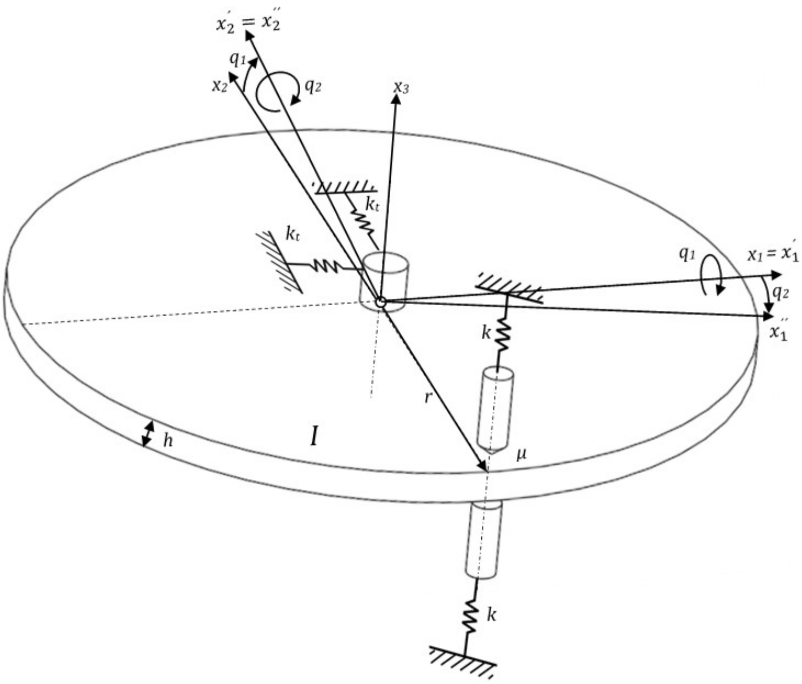

Figure 1. Minimal model of rigid brake disc including friction force between the pads and wobbling disc.

The parameter I represents the inertia momentum of the rigid disc to the axis x_1, and x_2, μ is friction coefficient, h is thickness of the disc, r is the radius of the disc and the distance of the pin-disc contact point to the center, N_0 is a prestress applied by pads on the disc, k_t is the stiffness coefficient of a bearing and k and is the stiffness coefficient of a pad. Stiffness matrix $\mathbf{K}$ in the equation (1) can by split into the symmetric matrix $\mathbf{K_s}$ and skew-symmetric matrix $\mathbf{K_{ss}}$ as introduced in [17]

$$\mathbf{K_s} = \mathbf{K_{disc}} + \mathbf{K_{pin}} + \mathbf{K_{friction}} \tag{3}$$

$$\mathbf{K_s} = \begin{bmatrix} k_t & 0 \\ 0 & k_t \end{bmatrix} + \begin{bmatrix} 2kr^2 + N_0 h & 0 \\ 0 & N_0 h \end{bmatrix} + \begin{bmatrix} 0 & \frac{1}{4}\mu N_0 \frac{h^2}{r} - \frac{1}{2}\mu(khr + 2N_0 h) \\ \frac{1}{4}\mu N_0 \frac{h^2}{r} - \frac{1}{2}\mu(khr + 2N_0 h) & \mu^2 h N_0 \end{bmatrix} \tag{4}$$

$$\mathbf{K_{ss}} = \begin{bmatrix} 0 & \frac{1}{4}\mu N_0 \frac{h^2}{r} + \frac{1}{2}\mu(khr + 2N_0 h) \\ -\frac{1}{4}\mu N_0 \frac{h^2}{r} - \frac{1}{2}\mu(khr + 2N_0 h) & 0 \end{bmatrix} \tag{5}$$

where the $\mathbf{K_{disc}}$ signifies the disc bearings stiffness contribution, $\mathbf{K_{pin}}$ pin stiffness contribution, and $\mathbf{K_{friction}}$ contribution of friction to symmetric stiffness matrix $\mathbf{K_s}$. The equation (4) represents a simple expansion of matrices in the equation (3).

 doi:10.20944/preprints202102.0114.v1

The stiffness proportional damping model (for $b_{q_1} = b_{q_2}$) is used to define the damping matrix **C** by following formula

$$\mathbf{C} = \beta\mathbf{K}\begin{bmatrix} b_{q_1} & 0 \\ 0 & b_{q_2} \end{bmatrix}, \tag{6}$$

where β represents the stiffness damping coefficient corresponding to the stiffness matrix **K** and b_{q_1}, b_{q_2} are general dimensionless proportionality damping factors, that are used to bring in non-proportionality of damping matrix to the system. Numerical values of minimal model are shown in Table 1.

Table 1. Numerical values of 2-DoFs model parameters.

$k_t(\frac{N}{m})$	$k(\frac{N}{m})$	$I(m^2)$	$\mu(-)$	$N_0(N)$	$h(m)$	$r(m)$	$\beta(-)$
5.4e3	9.3e3	4e-6	0.58	4000	0.037	0.11	1.5e-7

System (1) is transformed to a $2n$ dimensional representation with state variable vector **y**

$$\mathbf{N}(\mu)\dot{\mathbf{y}} + \mathbf{P}(\mu)\mathbf{y} = \mathbf{0} \tag{7}$$

where

$$\mathbf{N}(\mu) = \begin{bmatrix} \mathbf{C}(\mu) & \mathbf{M} \\ \mathbf{M} & \mathbf{0} \end{bmatrix}, \mathbf{P}(\mu) = \begin{bmatrix} \mathbf{K}(\mu) & \mathbf{0} \\ \mathbf{0} & -\mathbf{M} \end{bmatrix}, \mathbf{y} = \begin{bmatrix} \mathbf{q} \\ \dot{\mathbf{q}} \end{bmatrix}. \tag{8}$$

2.2. Results

Eigenvalues of system (7) are computed according to the [21]. The system is initialized using parameters introduced in Table 1 and the eigenfrequencies of this undamped non-stable system equals 6003 Hz. The minor difference between the values of eigenfrequencies appears firstly on the third decimal number. The Monte Carlo method is employed to create the stability region of given model and to analyze the influence of non-proportional damping matrix **C** controlled by parameters b_{q_1} and b_{q_2} on the stability of the model (1). The stability graph is shown on Figure 2.

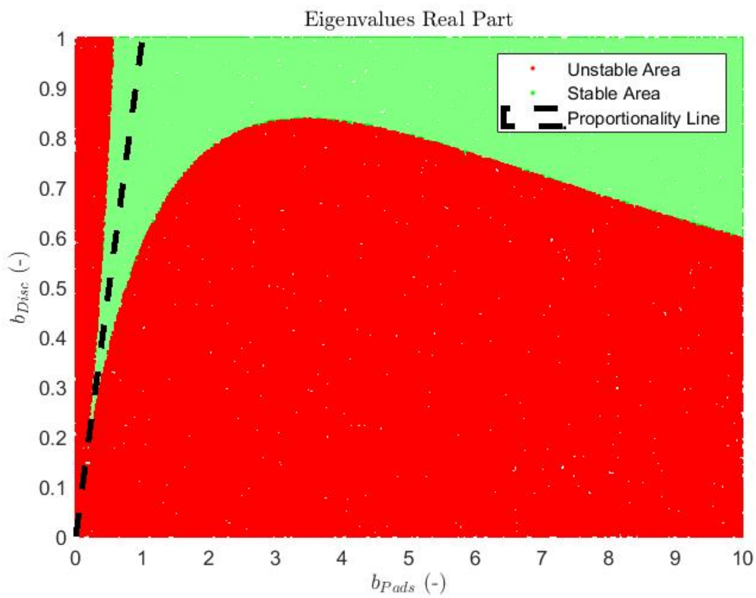

Figure 2. Influence of the damping matrix structure on stability of the break disc model. Structure of damping matrix is changed by two dimensionless parameters. Red zone - unstable systems, Green zone - stable systems, Black dashed line - the proportionality line.

Preprints (www.preprints.org) | NOT PEER-REVIEWED | Posted: 3 February 2021 doi:10.20944/preprints202102.0114.v1

Figure 2 contains the relation between the proportionality damping factors b_{disc} and b_{pad}. The stability is evaluated based on the maximum of real part value of both eigenvalues. Red zone represents systems with non-stable behavior and with positive real part of at least one eigenvalue of the system. Green zone contains the stable systems with negative real parts and the black line is a proportionality line. The proportionality line represents the set of systems with proportional damping matrix **C** to the stiffness matrix **K**. At small damping the system behaves non-stable. Increasing the damping proportionally would cause the system entering the stability region near the proportionality line (black dashed line in Figure 2). Obviously, increasing the non-proportionality at first or at second degree of freedom would cause the loss of stability in both direction.

3. Pad-on-disc system description

A complex model of disc brake is considered in the form of the pad-on-disc system, shown in Figure 3a. The physical principle of the operation of the experimental device is as follows. The friction material 8 is pressed against the rotating discs 9 through the thin plate 7. Due to the rotation of the brake disc 9 and the friction forces F between the brake disc 9 and the friction material 8, the friction material 8 is tilted as shown in Figure 3b. From the point of view of arrangement dynamics, nonconservative frictional forces cause a dynamic instability and lead into brake squeal. Basic dimensions of system

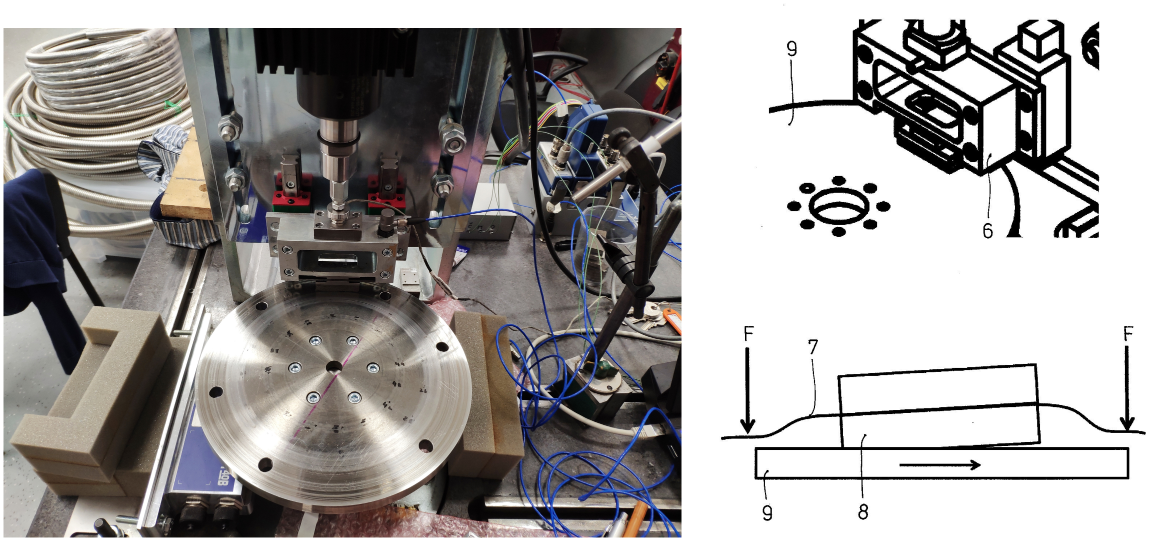

(a) **(b)**

Figure 3. a) pad-on-disc experimental test bench b) working principle of pad-on-disc, 6 – pad support, 7- thin plate, 8 – friction material, 9 – disc.

components are collected in Table 2.

Table 2. Basic dimensions of pad-on-disc system components: ϕD_D - disc diameter, t_D - disc thickness, l - friction material (FM) length, w - FM width, h - FM height, ϕD_H - hub diameter, t_t - thin plate thickness

ϕD_D(mm)	t_D (mm)	l (mm)	w (mm)	h (mm)	ϕD_H (mm)	t_t (mm)
215	14	40	20	8	108	2

 doi:10.20944/preprints202102.0114.v1

3.1. *Analyses of brake squeal on simplified experimental brake model*

For analyses of modal content of the given system, Frequency Response Function (FRF) measurement has been performed on free as well as mounted and loaded disc. Measurements reveal possible modes as candidates for mode coupling leading to squeal. Measurements were performed by modal hammer and accelerometer sensors placed on the disc structure.

Performing Fast Fourier Transform (FFT) on multiple measured signals, the multiple FRFs was obtained from time signals and their averaged value for the free disc is shown in Figure 4a. The numbers in brackets (d,c) represent a number of nodal diameters and a number of nodal circles of a given mode. Three bending modes of three, four, and five nodal diameters have been identified using experimental modal analyses.

Figure 4b shows detail of FRF, for clamped and loaded disc, around a couple of (4,0) modes which are considered as most prone to be coupled. Different FRF evolution with different loading can be seen. Modes are receding from each other and their damping ratio changes with increasing load. This is due to decreasing the symmetricity of the disc structure by adding the pad structure into it and introducing additional damping by friction material as well as frictional contact between the friction material and the disc.

The characteristic squeal frequency of the studied system occurs in the region of 5800Hz - 6000Hz, depending on physical conditions like temperature, contact pressure distribution between the friction material and the disc as well as fiction intensity. The typical measurement of squeal frequency, taken using two accelerometer sensors placed on a slowly rotating disc structure is shown in Figure 5.

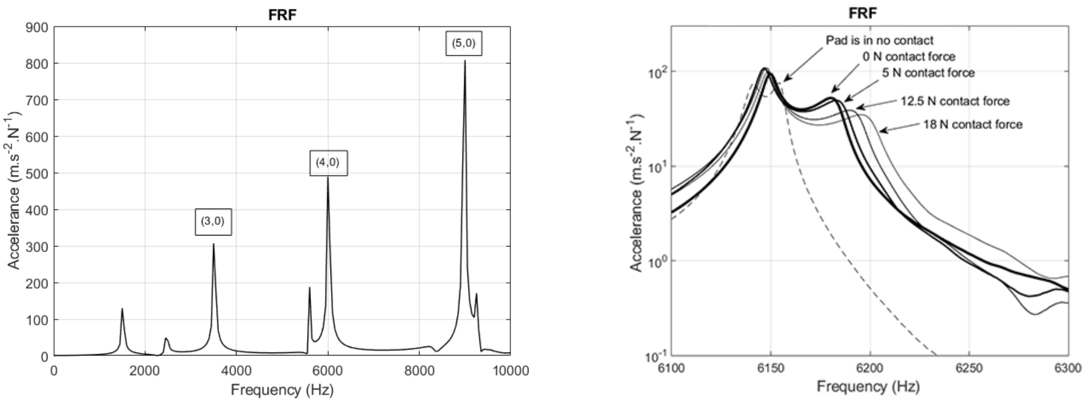

(a) **(b)**

Figure 4. a) Averaged FRF of the free disc with highlighted modeshapes, b) comparison of FRF for different pad loading variations in 5800-6200 Hz region.

3.2. *Mathematical description of pad-on-disc system*

Since experimental analyses of structural damping impact on squeal is a complicated task and behind the scope of this study, the numerical calculations of brake squeal have been adopted. The Finite Element Method (FEM) is used to define a mathematical model of given physical problem. FEM discretization results in the system of equations of motion with constant coefficient matrices. System stability can be studied using a solution of the general eigenvalue problem in the same way as it was in the case of the simple 2DoFs system in previous chapters.

Geometry of the system is shown in Figure 6a and its FEM representation in Figure 6b. All calculations are realized in Ansys 2020R1 software.

The FE model is defined and its modal properties are tuned following the experimental modal analyses on a physical model. Numerical value of damping ratio $\zeta_i = 0.4\%$ of the disc made of

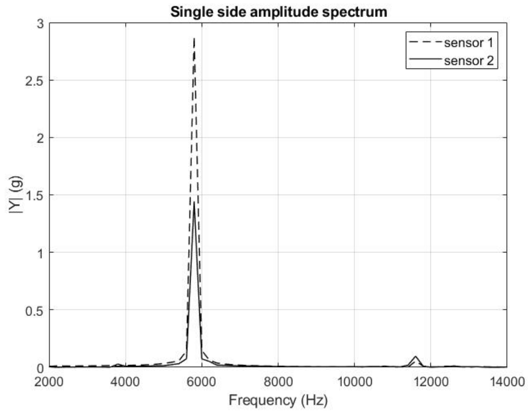

Figure 5. Single side amplitude spectrum of measured squeal signal [21].

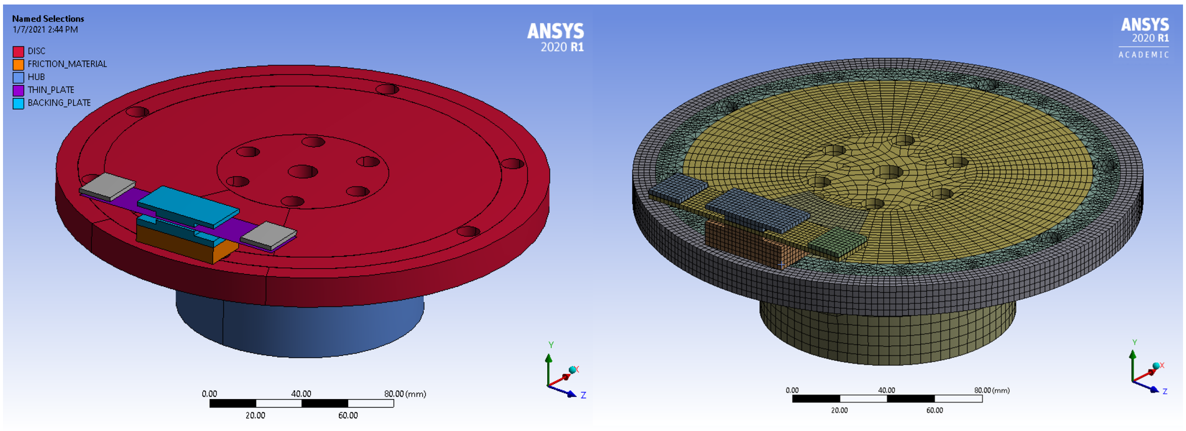

(a) **(b)**

Figure 6. a) Geometry of the simplified pad-on-disc brake model, b) FEM representation of the model counting 75520 elements and 184225 nodes.

structural steal has been determined from FRF measurements for couple of potentially unstable (4,0) modes.

In ANSYS FEM code, the material-dependent damping can be modeled directly through damping ratio or can be represented by Rayleigh damping factors as it was in this study. Rayleigh damping factors, α, β applied into FE material model have been determined from the equations

$$\zeta = \frac{1}{2}\left(\frac{\alpha}{\omega} + \beta\omega\right), \tag{9}$$

$$\left(\frac{d\zeta}{d\omega}\right)_{\omega=\omega_i=\omega_{i+1}} = 0. \tag{10}$$

Under the assumption that the single components are proportional damped and their damping ratios ζ_i of i-th and $(i+n)$-th modes are known, then for a couple of two modes and their corresponding eigenfrequencies, two equations of two unknown factors α and β can be obtained from (9). In the case of a symmetric disc structure, the studied couple of eigenfrequencies, related to unstable (4,0) mode shape, are assumed to be $\omega = \omega_i = \omega_{i+1}$ and their damping ratios $\zeta = \zeta_i = \zeta_{i+1}$. In this case unknow coefficients are calculated satisfying the equations (9), (10) as $\alpha = \zeta_i\omega_i$ and $\beta = \zeta_i/\omega_i$.

Damping ratio value for non-asbestos organic type friction material containing novolac resin as binder and also various ingredients including metallic fillers can vary according to composition from

2% to 5% [15]. The damping ratios of the remaining materials in the model are considered to be the same as for the disc component. In Table 3 the list of all used material parameters is shown.

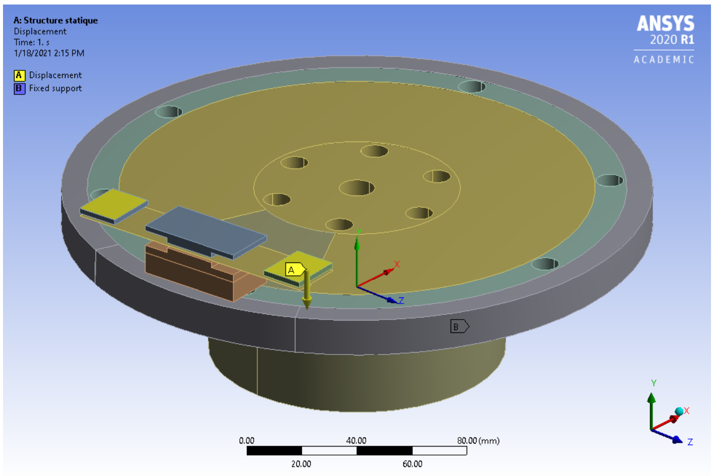

Figure 7. Boundary conditions for static equilibrium analysis.

Using FE approximation of a given continuous physical system, the behavior of the system around its equilibrium position can be described by a finite set of differential equations with time-independent coefficient matrices. The static equilibrium position is achieved by prestressing nonlinear static analysis. Loading of the system is achieved by boundary conditions as it is defined in Figure 7. The bottom area of the hub is fixed while on the square yellow areas of the thin plate displacement of the value 8e-2mm, corresponding to the reaction force of 200N, is applied. After the equilibrium position is achieved, the pseudo rotation of the disc using the Ansys "CMROTATE" command is being applied in a further step of the analysis. This command sets the constant rotational velocity on the nodes of the disc element component, despite any deformation at the nodes. This feature is primarily used for generating sliding contact at frictional contact interfaces in a brake-squeal analysis. Due to the sliding contact, the unsymmetric coefficient matrices, in the linear differential equations set (11) are obtained.

$$\mathbf{M}\ddot{\mathbf{q}} + [\mathbf{C} + \mathbf{C_{ns}}(\mu)]\dot{\mathbf{q}} + [\mathbf{K} + \mathbf{K_{ns}}(\mu)]\mathbf{q} = \mathbf{0} \tag{11}$$

The terms $\mathbf{K_{ns}}(\mu)\mathbf{q}$ and $\mathbf{C_{ns}}(\mu)\dot{\mathbf{q}}$ represent the nonconservative friction forces. The matrices $\mathbf{K_{ns}}$ and $\mathbf{C_{ns}}$ are nonsymmetric and smoothly depend on friction parameter μ. Symmetric positively definite matrices $\mathbf{C}$ resp. $\mathbf{K}$ represent a system structural damping resp. stiffness. The matrix $\mathbf{C}$ is modeled non-proportionally to $\mathbf{K}$ and $\mathbf{M}$ matrices, due to the definition of different material damping for friction material and the rest of the assembly. Gyroscopic effects are neglected in this study.

For further analyses of the system stability, complex eigen values λ_i and corresponding complex displacement eigenvectors $\boldsymbol{\psi}_{\mathbf{D}i}$ of original system (11) are obtained by solution of the eigenvalue problem (12) and transformation of complex eigenvector $\tilde{\boldsymbol{\psi}}_i$ from modal into generalized coordinates (14)

$$(\mathbf{A} - \lambda_i \mathbf{I})\tilde{\boldsymbol{\psi}}_i = \mathbf{0}, \tag{12}$$

$$\mathbf{A} = \begin{bmatrix} \mathbf{0} & \mathbf{I} \\ -\boldsymbol{\Omega}^2 - \boldsymbol{\Phi}^\top \mathbf{K_{ns}} \boldsymbol{\Phi} & -\boldsymbol{\Phi}^\top (\mathbf{C} + \mathbf{C_{ns}})\boldsymbol{\Phi} \end{bmatrix}, \tag{13}$$

$$\boldsymbol{\psi}_{\mathbf{D}i} = \boldsymbol{\Phi}\mathbf{T}\tilde{\boldsymbol{\psi}}_i, \mathbf{T} = [\mathbf{I}, \mathbf{0}]. \tag{14}$$

The modal $\boldsymbol{\Phi} = \{\boldsymbol{\phi}_i\}$, and the spectral $\boldsymbol{\Omega}^2 = diag\{\omega_i^2\}$ matrixes are obtained by solving the generalized eigenvalue problem

$$(\mathbf{K} - \omega_i^2 \mathbf{M})\boldsymbol{\phi}_i = \mathbf{0}. \tag{15}$$

 doi:10.20944/preprints202102.0114.v1

Table 3. Material properties used in the complex eigenvalues calculation.

Friction material						
T(°C)	ρ(kg/m^3)	E_x (Pa)	E_y (Pa)	E_z (Pa)	$\nu_{xy}(-)$	$\nu_{yz}(-)$
23	2930	8.7e09	8.7e09	2.5e09	0.24	0.1
100	2930	5.9e09	5.9e09	1.7e09	0.24	0.1
	$\nu_{xz}(-)$	G_{xy}(Pa)	G_{yz}(Pa)	G_{xz}(Pa)	$\zeta_p(\%)$	
23	0.35	3.5e09	1.6e09	1.6e09	0-10 (5)*	
100	0.35	2.4e09	1.1e09	1.1e09	0-10 (5)*	
Disc						
T(°C)	ρ(kg/m^3)	E (Pa)	$\nu(-)$	$\zeta_d(\%)$		
23	7683	1.9e11	0.25	0-0.8 (0.4)*		
Thin plate, Backing plate, Hub						
T(°C)	ρ(kg/m^3)	E (Pa)	$\nu(-)$	$\zeta(\%)$		
23	7800	2.1e11	0.3	0.4		

* default value

3.3. Results

From the set of calculated eigenvalues, corresponding to the region of interest 0 - 10 kHz and for default material properties, two unstable modes characterized by positive real part of their eigenvalues were identified. Their mode shapes are shown in Figure (8). The first unstable mode corresponds with experimental measurements (Figure 5).This mode results from coupling of two neighbouring (4,0) disc bending modes. Since the second calculated unstable mode cannot be experimentally verified, it is considered to be over prediction. This mode results from coupling of two (5,0) disc bending modes.

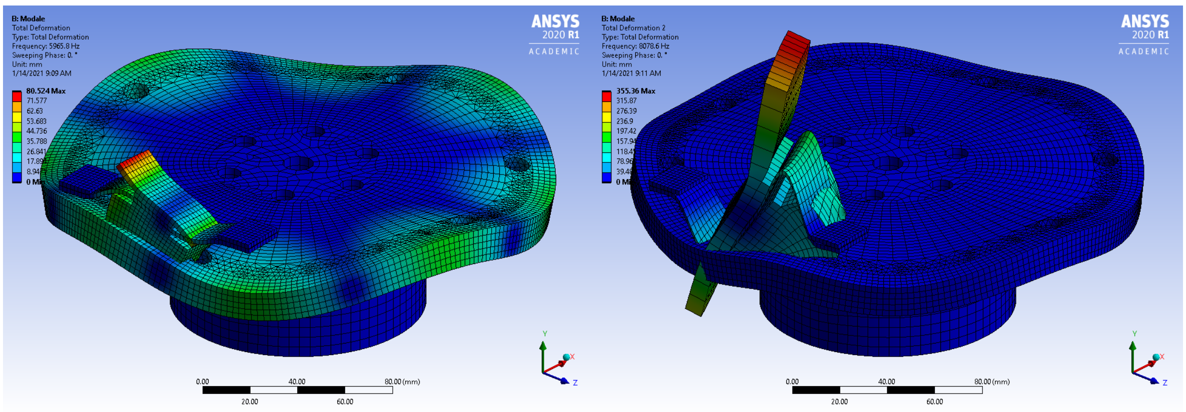

(a) (b)

Figure 8. Calculated unstable mode shape of the system at a) 5966 Hz (experimentally verified), b) at 8079 Hz (over predicted)

Stability sensitivity to change the damping of disc and friction material is studied further for the first, experimentally verified, unstable mode. The full factorial numerical experiment counting 49 simulations, evaluated for different values of material depended damping of the disc and the friction material component reveals the system stability regions. Intervals of used damping ratio values in this study can be found in Table 3. Figure 9a shows maximum of all calculated real parts of eigenvalues λ for different damping ratios of the disc ζ_d and the friction material ζ_p. Green surface separates stable and unstable solutions, where all solutions above this surface are unstable whereas all solutions below the surface are stable.

Preprints (www.preprints.org) | NOT PEER-REVIEWED | Posted: 3 February 2021 doi:10.20944/preprints202102.0114.v1

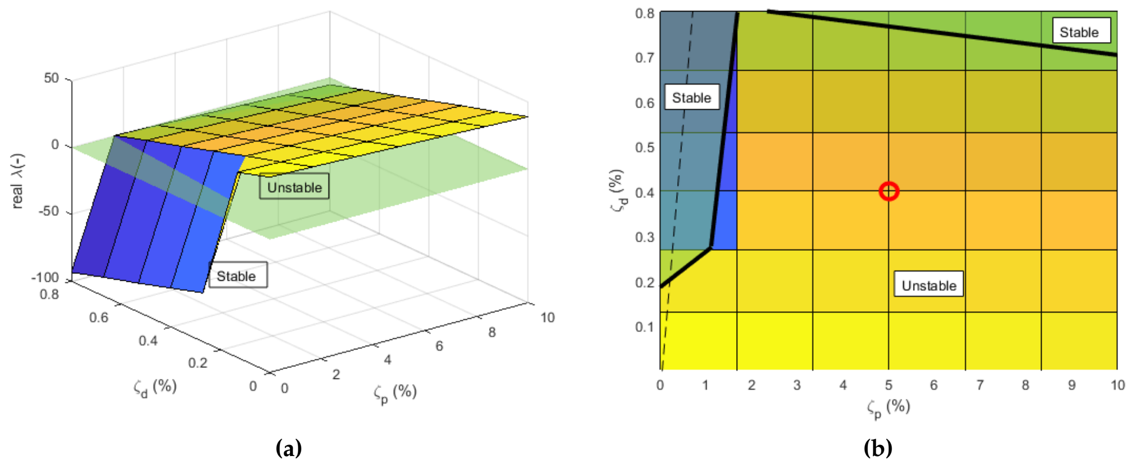

Figure 9. a) Stability map with respect to ζ_d, ζ_p damping ratios, b) stability map in the ζ_d - ζ_p plane. Bold lines – stability boundary, dashed line – proportional damping line, red circle – default damping ratio values.

Figure 9b shows a 2D detailed view of the obtained stability areas. Solid lines represent the boundary between stable and unstable areas. The dashed line represents a proportionally damped system, where the damping of the disc ζ_d and the friction material ζ_p has the same values. The red dot on the graph represents the default damping for the disk and friction material. The results show that the behaviour of the system with the default damping is in an unstable area. If the system were proportionally damped, it would be stabilized at damping ratio value of about $\zeta_d = \zeta_p = 0.2\%$ and increasing it would make the system more stable, which is in line with the theory of proportional damping playing purely stabilising role in the non-conservative systems. Based on the actual situation, the given system and the given unstable mode could be stabilized by a suitable adjustment of the damping of the friction material and the disc. If the damping of the disc was maintained, the damping of the friction material would have to be reduced to bring the system into a stable area. If the damping ratio of the friction material was reduced below $\zeta_p = 1.5\%$, the system would become stable, which is contra intuitive. If constant friction material damping were considered, the disc damping would have to reach a value of almost $\zeta_d = 0.8\%$ for the system to be stable.

4. Conclusion

The paper aims to study the effect of damping on the stability of the particular disc brake system and to assess the importance of components damping concerning stability and thus brake squeal. The analysis is performed by a simplified (2 Dof) as well as a complex (multiple DoF) models of a disc brake. It has been stated in the work of various authors as well as in the classical theory of vibration of mechanical systems that in the case of non-conservative systems, damping can play both a stabilizing as well as destabilizing role.

Both analyzed models show the dependence of stability on the degree of proportionality of damping. At low damping levels, the systems show unstable behavior. Increasing the damping while maintaining its proportionality stabilizes the system ultimately. However, this does not apply in the case of a deviation from proportional damping, where increasing the damping of one part of the structure at the expense of another, can lead to destabilization. Since both models show this action, regardless of the complexity, it implies that similar behavior can be anticipated in commercial disc brake systems. From the given observation can be concluded that an effective brake squeal prediction process should account for damping.

Concerning the questions defined in the introduction, both can be answered positively. Non-proportional damping can have a significant influence on the stability of disc brake systems. This study is pointing to the fact, that disc brake systems can contain unstable modes which are for common material properties prone to be destabilized by dissipation induced instability. However, it cannot be concluded, from the scope of this research, that all unstable modes are sensitive in this manner for physically reasonable material properties, especially damping propensity.

Non-proportional damping can be modeled in modern FEA tools using material-dependent damping models. By definition of specific material-dependent damping, for single components, it leads to a non-proportional damping matrix relative to mass and stiffness matrices of a system. This allows appraising unstable system modes sensitivity to damping.

In further research, the team of authors wants to focus on two main goals. The first goal is to examine other unstable, experimentally verifiable, modes of the system to determine the degree of their sensitivity to the proportionality of the damping. The second goal is an experimental verification of numerically obtained results in this study by preparation of mixtures of friction material leading to various damping. If this research was experimentally verified, it would help to extend common brake squeal prediction tools about damping modeling and design, to prevent brake squeal more effectively.

Funding: This research was funded by the Grant Agency of the Slovak Academy of Sciences (VEGA 1/0227/19 - Extension of current prediction methods for car disc brake dynamic instability including thermal-structural effects.

References

1. Kirillov, O. N. Nonconservative Stability Problems of Modern Physics, In *De Gruyter Studies in Mathematical Physics 14*; De Gruyter: Berlin, Germany, 2013.
2. van der Meer, J. Hamiltonian Hopf Bifurcation, In *Lecture Notes in Mathematics 1160*; Springer-Verlag: Berlin, Germany, 1985.
3. Kollár, R. and Miller, P. D. Graphical Krein signature theory and Evans-Krein functions. *SIAM Review* **2014**, *56*, *1*, 73–123.
4. Nackenhorst, U. and Brinkmeier, M. On the dynamics of rotating and rolling structures. *Archive of Applied Mechanics* **2018**, *78*, *6*, 477–488.
5. Diana, G.; Rocchi, D.; Argentini, T. and Muggiasca, S. Aerodynamic instability of a bridge deck section model: Linear and nonlinear approach to force modeling. *Journal of Wind Engineering and Industrial Aerodynamics* **2010** , *98*,*6–7*, 363–374.
6. Altmeyer, S.; Hoffmann C. and Lücke, M. Islands of instability for growth of spiral vortices in the Taylor-Couette system with and without axial through flow. *Physical Review E* **2011**, *84*, *4*, 046308.
7. Kinkaid, N. M.; O'Reilly O. M. and Papadopoulos P. Automotive disc brake squeal. *Journal of Sound and Vibration* **2003**, *267*, *1*, 105–166.
8. Sergienko, V. P. and Bukharov, S. N. Noise and Vibration in Friction Systems. *Springer International Publishing Switzerland* **2015**, *212*.
9. Ibrahim, R. A. Friction-induced vibration, chatter, squeal and chaos, part II: dynamics and modelling. *ASME Applied Mechanics Reviews* **1994**, *47*, *7*, 227–253.
10. Kang, J.; Nam, J. Minimal Model for Sprag-Slip Oscillation as Catastrophe-Type Behavior. Appl. Sci. 2020, 10, 2748. https://doi.org/10.3390/app10082748
11. Hoffmann, N.; Fischer, M.; Allgaier, R. and Gaul L. A minimal model for studying properties of the mode-coupling type instability in friction induced oscillations. *Mechanics Research Communications* **2002**, *29*, *4*, 197–205.
12. Smith, D. M. The motion of a rotor carried by a flexible shaft in flexible bearings. *Proceedings of the Royal Society of London. Series A, Containing Papers of a Mathematical and Physical Character* **1933**, *142*, *846*, 92–118.
13. Bajer, A.; Belsky, V.; and Kung, S. The Influence of Friction-Induced Damping and Nonlinear Effects on Brake Squeal Analysis. *SAE Technical Paper 2004-01-2794*, **2004**, https://doi.org/10.4271/2004-01-2794.
14. Abu-Bakar, R. A. and Ouyang, H. Complex eigenvalue analysis and dynamic transient analysis in predicting disc brake squeal. *International Journal of Vehicle Noise and Vibration* **2006**, *2*, *2*, 143-–155.

15. Masoomi, M.; Katbab, A.A. and Nazockdast, H. Reduction of Noise from Disc Brake Systems Using Composite Friction Materials Containing Thermoplastic Elastomers (TPEs). *Appl Compos Mater 13*, 305-–319, https://doi.org/10.1007/s10443-006-9018-7.
16. Beards, C.F. Structural Vibration: Analysis and Damping; Arnold, London, Sidney, Auckland, 1996.
17. Hagedorn, P.; Eckstein , M.; Heffel E.; Wagner, A. Self-Excited Vibrations and Damping in Circulatory Systems. *Transactions of the ASME, Journal of Applied Mechanics* **2014**, *81*, *10*, 101009-1-–101009-9.
18. Wehner, J.H.; Jekel, J.; Sampaio, R.; Hagedorn, P. Damping Optimization in Simplified and Realistic Disc Brakes, In *SpringerBriefs in Applied Sciences and Technology*; Kacprzyk J., Ed,; Springer International Publishing, 2018.
19. Ungar, E.E.; Zapfe, J.A. Structural damping., In *Noise and Vibration Control Engineering*; Vér, I.L., Ed.; Wiley: Hoboken, USA 1965.
20. von Wagner, U.; Hochlenert, D.; Hagedorn, P. Minimal models for disk brake squeal. *Journal of Sound and Vibration* **2007**, *3*, 527-–539, https://doi.org/10.1016/j.jsv.2006.11.023.
21. Úradníček, J.; Musil, M. and Bachratý, M. Frequency response function measurement on simplified disc brake model. *Strojnícky časopis : Journal of Mechanical engineering* **2018**, *68*, *3*, 225–230.